

# Half-metallicity and efficient spin injection in AlN/GaN:Cr (0001) heterostructure

J. E. Medvedeva<sup>1</sup>, A. J. Freeman<sup>1</sup>, X. Y. Cui<sup>2</sup>, C. Stampfl<sup>2</sup> and N. Newman<sup>3</sup>

<sup>1</sup> *Physics and Astronomy Department, Northwestern University, Evanston, Illinois 60208-3112*

<sup>2</sup> *School of Physics, University of Sydney, Sydney, Australia*

<sup>3</sup> *Chemical and Materials Engineering Department, Arizona State University, Tempe, Arizona 85287-6006*

First-principles investigations of the structural, electronic and magnetic properties of Cr-doped AlN/GaN (0001) heterostructures reveal that Cr segregates into the GaN region, that these interfaces retain their important half-metallic character and thus yield efficient (100 %) spin polarized injection from a ferromagnetic GaN:Cr electrode through an AlN tunnel barrier – whose height and width can be controlled by adjusting the Al concentration in the graded bandgap engineered  $\text{Al}_{1-x}\text{Ga}_x\text{N}$  (0001) layers.

PACS numbers: 71.20.-b, 73.20.-r, 75.70.Cn, 85.75.-d

The injection and manipulation of spin polarized carriers – a key feature determining successful spintronics – is highly dependent on phenomena and processes occurring at the interface between a ferromagnet and a semiconductor. It has been shown<sup>1–3</sup> that surface or interface sensitive approaches must be employed in both theory and experiment for the accurate determination of the spin polarization in materials proposed for potential magnetoelectronic devices. As perhaps the most striking example, Heusler compounds (such as NiMnSb,  $\text{Co}_2\text{MnGe}$ ,  $\text{Co}_2\text{CrAl}$ ) – which possess the appealing half-metallic ferromagnetic behavior in bulk – show significantly reduced spin polarization at the surface<sup>2</sup> or, consequently, at the interface with a semiconductor<sup>3</sup>. Indeed, first-principles calculations have revealed that structural reconstruction in the vicinity of the junction essentially alters the electronic states and destroys half-metallicity<sup>3</sup>.

Recently, nitride-based semiconductors, in particular GaN and AlN, have attracted increasing attention for a number of reasons: (i) The introduction of magnetic dopants and achieving ferromagnetism in these materials provide complementary functionality to the wide range of devices already developed for pure large band-gap nitrides<sup>4</sup>. (ii) The shorter bond length and smaller spin-orbit coupling in these light-element compounds as compared to other III-V semiconductors (e.g., GaAs) are predicted to give rise to higher Curie temperatures<sup>5</sup>; indeed, recent measurements in Cr-doped GaN and AlN bulk showed  $T_c$  to be over 900 K<sup>6</sup>. (iii) The smaller spin-orbit interaction is also one of the main arguments for longer (by three orders of magnitude) electron spin lifetimes in GaN than in GaAs<sup>7</sup>. (iv) The III-N semiconductors appear to be much more resilient to the presence of extended structural defects than are other semiconductors<sup>8</sup>. While Cr-doped bulk GaN and AlN systems have been extensively studied<sup>6,9–11</sup>, both experimental investigations and theoretical modeling of magnetically doped III-N interfaces – essential for practical spintronic applications – are lacking.

In this Letter, we present results of first-principles calculations of Cr-doped AlN/GaN (0001) heterostructures focusing on their structural, electronic and magnetic properties. From a comparison of the formation

energy of the relaxed AlN/GaN heterostructures with different site locations of Cr, we predict that the magnetic impurity segregates into the GaN region which serves as a ferromagnet, while AlN is the semiconductor part of the interface. Most significantly, we find that the Cr-doped nitride-based interface retains the desired half-metallic behavior that enables the efficient 100 % spin polarized injection across the interface and thus makes this system highly attractive for spintronic applications. Finally, we propose a way to control the shape (i.e., height and width) of the nitride potential barrier by adjusting the concentration  $x$  in a Cr-doped interface with a graded  $\text{Al}_{1-x}\text{Ga}_x\text{N}$  barrier region – a realistic magnetoelectronic structure that can be grown epitaxially.

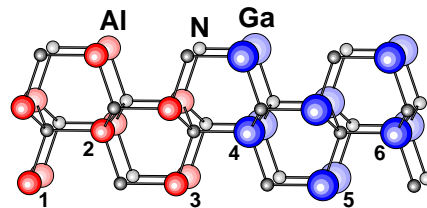


FIG. 1. Geometry of (2x2) AlN/GaN (0001) heterostructure: the large, intermediate and small spheres correspond to Ga, Al and N atoms, respectively. Substitutional site locations of Cr atoms in the supercell denoted by numbers.

The AlN/GaN (0001) interface is modeled using (1x1), (2x2) and (2x4) supercells of pure or Cr-doped wurtzite GaN and AlN (0001) with 3 double layers of each material, cf. Fig. 1. Note that a “double layer” is a single nitride layer, i.e., it consists of a group III element and nitrogen, so the (1x1), (2x2) and (2x4) supercells contain 12, 48 and 96 atoms, respectively. For the  $\text{Al}_{1-x}\text{Ga}_x\text{N}$ /GaN (0001) heterostructures, we used (2x2) supercells with  $x=0.00, 0.25, 0.50, 0.75$  and 1.00 in the layers, i.e., the content of Al (Ga) gradually decreases (increases) along the (0001) direction until a composition of pure GaN is formed. The equilibrium relaxed geometry of the structures was determined via total energy and atomic forces minimization for the lattice parameters  $a$  and  $c$  and the internal parameter  $u$ . Both the GaN and

AlN regions of the heterostructure were allowed to relax with the same in-plane lattice constant<sup>12</sup>, while the internal atomic relaxation for each lattice parameter  $c$  provided different minimized III–N distances along the (0001) direction. Note, that during the optimization, *all* atoms were allowed to move in the  $x$ ,  $y$  and  $z$  directions.

TABLE I. Calculated lattice parameters, Å, and band gap values, eV, for bulk wurtzite AlN and GaN and for the AlN/GaN (0001) heterostructure. Experimental data are taken from Ref. 16.

	Lattice parameters				Band gap		
	$a$	$c$	$a_{exp}$	$c_{exp}$	LDA	sX-LDA	Exp.
AlN	3.085	4.993	3.112	4.982	4.34	6.05	6.20
GaN	3.142	5.194	3.189	5.185	2.00	3.35	3.39
AlN/GaN	3.127	15.402			2.59	3.98	

We employ the all-electron full-potential linearized augmented plane wave (FLAPW) method<sup>13</sup> that has no shape approximation for the potential and charge density. Cut-offs of the plane-wave basis (16.0 Ry) and potential representation (81.0 Ry), and expansion in terms of spherical harmonics with  $\ell \leq 8$  inside the muffin-tin spheres were used. Summations over the Brillouin zone were carried out using 32 special  $\mathbf{k}$  points in the irreducible wedge. In addition to the local density approximation (LDA) for the ground state properties, we used the self-consistent screened-exchange LDA (sX-LDA) method<sup>14,15</sup>, which is known to provide a considerably improved description of the excited state (optical) properties as compared to the LDA or generalized gradient approximation (GGA) calculations.

We first determine the effect of the interface on the structural and electronic properties of pure AlN/GaN (0001) and compare with those of bulk GaN and AlN. Due to the lattice mismatch, both GaN and AlN are found to be mutually strained in the junction, cf. Table I: (i) The resulting in-plane lattice constant, 3.127 Å, is 0.5 % smaller (1.3 % larger) than that of the bulk GaN (AlN) and is in agreement with the value observed<sup>12</sup> for the thinnest AlN/GaN bilayer, 3.134 Å. (ii) The renormalized  $c$  lattice constant of GaN in the heterostructure is larger than that of AlN by 0.195 Å which is approximately equal to the difference between the  $c$  parameters of the bulk materials, cf., Table I. We also found that away from the junctions, the Ga–N and Al–N distances along (0001) in each sub-unit tend to relax back towards their unstrained bulk values and differ by 0.7 % (0.9 %) from those in the bulk GaN (AlN). Further, the structural relaxation at the junctions affects the electronic properties, in particular, the optical bandgap of AlN/GaN (0001). In Table I, we present the bandgap values of bulk GaN and AlN and the (1x1) AlN/GaN (0001) calculated using both the LDA and sX-LDA methods. As expected, the LDA underestimates the band gap of both bulk GaN and AlN by 30–40 %, while the sX-LDA

gives a considerably improved description – namely, a less than 2%-difference from the experimental values. For the AlN/GaN (0001), we found that the valence band maximum and the conduction band minimum are formed by states of the GaN layers; thus, these states determine the calculated minimum band gap of the system to be 2.59 eV (3.98 eV) within the LDA (sX-LDA). In contrast, the states of the AlN layer located further away from the junctions lie deeper in the valence and conduction bands giving a bandgap increase of  $\sim 0.4$  eV within both the LDA and sX-LDA<sup>17</sup>.

Next, we investigated the effect of the interface on the transition-metal impurity location and the magnetic properties of the doped structure. To this end, we performed calculations of Cr doped substitutionally into the (2x2) AlN/GaN (0001). (For comparison of the electronic and magnetic properties, we also calculated Cr-doped bulk GaN and AlN.) The choice of the (2x2) supercell is motivated by the recently calculated critical separation between two Cr atoms in bulk GaN,  $\sim 2.7$  Å, above which ferromagnetic (FM) coupling dominates the antiferromagnetic (AFM) one<sup>11</sup>. In our supercell case, the Cr–Cr distance is 6.3 Å. Now, to find the preferred site location of the magnetic impurity, we calculated the formation energies<sup>18</sup> of six relaxed structures with cation-substituted Cr, cf. Fig. 1. The results, gathered in Table II, allow the following conclusions:

TABLE II. Comparison of the calculated formation energies, eV, and the magnetic moments on the Cr atoms and its tetrahedral N neighbors in plane ( $N_{planar}$ ) and along the (0001) direction ( $N_{apical}$ ),  $\mu_B$ , for the Cr-doped (2x2) AlN/GaN (0001) heterostructures. Site locations of the Cr atoms (in parentheses) correspond to those in Fig. 1.

	AlN region			GaN region		
	Cr(1)	Cr(2)	Cr(3)	Cr(4)	Cr(5)	Cr(6)
$\Delta E_f$	+1.825	+1.817	+1.827	0.000	+0.031	+0.010
Cr	2.309	2.309	2.308	2.302	2.304	2.299
$N_{planar}$	−0.010	−0.011	−0.015	−0.020	−0.019	−0.016
$N_{apical}$	−0.018	−0.007	−0.005	−0.003	−0.012	−0.012

(i) The magnetic impurity segregates into the GaN region of the heterostructure which serves as a ferromagnet (as shown below), while the AlN region is a non-magnetic part of the interface. The difference of the formation energies for Cr in the AlN and in the GaN region of the heterostructure ( $\sim 1.8$  eV, cf. Table II) shows little dependence on the distance from the junctions<sup>19</sup> and agrees well with that for Cr-doped bulk GaN and AlN (2.0 eV).

(ii) Although the calculated local magnetic moments on the Cr atoms in the AlN/GaN, Table II, are similar to those obtained for the corresponding relaxed Cr-doped bulk GaN (2.304  $\mu_B$ ) and AlN (2.313  $\mu_B$ ), the presence of the junctions does affect the magnetic properties of the system. This can be seen from a comparison of the induced magnetic moments on the tetrahedral N neighbors

of the Cr atom (i.e., three in-plane N and one apical N atoms, cf. Fig. 1), presented in Table II. We found that the magnetic moments are larger on the N atoms which bond with Ga than on those connected to Al atoms by  $0.006 \mu_B$  (or  $0.009 \mu_B$ ) for planar (or apical) N atoms, on average. This finding can be explained by the fact that the states of the AlN layers lie deeper in the valence band (as discussed above) and hence they are more screened as compared to the GaN layers<sup>20</sup>. Therefore, at the junction where the in-plane N atoms bond with Ga and the apical N atom bonds with Al, the induced in-plane spin polarization is dominant (case 4, Table II). In contrast, a higher spin polarization along (0001) – as compared to the in-plane magnetic moments – is observed at the other junction (case 1, Table II). Accordingly, we found the magnetic moments on planar and apical N atoms to be similar when Cr is equidistant from the junctions.

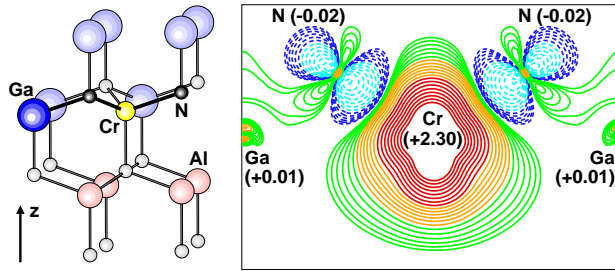


FIG. 2. Geometry of the most energetically favorable Cr site location in the AlN/GaN (0001) heterostructure (left) and contour plot of the calculated spin density distribution within a slice passing through this Cr atom and its planar N neighbors (right). Solid (dash) lines in the plot denote positive (negative) spin polarization. The calculated magnetic moment on the atoms,  $\mu_B$ , is given in parentheses.

A contour plot of the calculated spin density distribution within a slice passing through the Cr atom and its planar N neighbors (case 4 in Table II) is presented in Fig. 2. In agreement with the itinerant *sp-d* exchange model<sup>21</sup>, the *p*-orbital of the N atoms which points toward the Cr atom has its magnetic moment antiparallel to the one on the magnetic impurity giving rise to FM coupling between two Cr atoms. (Note, that the other two N *p*-orbitals possess positive spin polarization and create hopping channels for itinerant electrons.) Indeed, from the (2x4) Cr-doped AlN/GaN (0001) supercell calculations, we confirm strong FM coupling between two Cr atoms with an energy difference between FM and AFM orderings of 97, 106 and 110 meV/Cr atom for case 4, 5 and 6, respectively. Accordingly, the effective exchange interaction parameters – estimated<sup>22</sup> to be 22, 26 and 28 meV, respectively – show a similar dependence on the Cr site locations, which correlates with the decrease of the ratio between the induced magnetic moments on planar and apical N atoms, cf. Table II.

(iii) Regardless of the Cr site location in the GaN region of the interface (cf. cases 4-6 in Table II with

a total energy difference of  $\sim kT$ ), the three Cr-doped AlN/GaN systems share similar band structure features (the corresponding band offsets are discussed in a separate paper<sup>23</sup>): The magnetic impurity *d* states hybridized with the *p* states of the neighboring N atoms form deep bands in the nitride bandgap, cf. Fig. 3. For the majority-spin channel, partially occupied triply degenerate  $t_{2g}$  and fully occupied doubly degenerate  $e_g$  bands are located at  $\sim 2.5$  eV and  $\sim 1.1$  eV, respectively, above the valence band maximum. The exchange interaction splits the Cr *d* states by  $\sim 2$  eV. These findings are in agreement with previous studies<sup>9,11</sup> of Cr-doped bulk GaN.

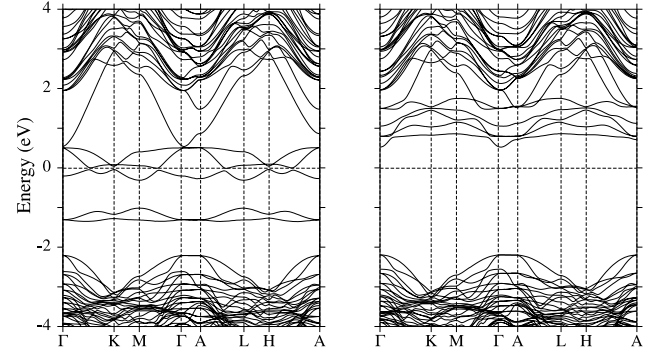


FIG. 3. Spin-resolved band structure along the high symmetry directions in the Brillouin zone for the most energetically favorable Cr-doped AlN/GaN (0001) heterostructure. The origin of the energy is taken at the Fermi level.

Most significantly, we found that the Cr-doped AlN/GaN (0001) heterostructures retain the desired half-metallic behavior (consistent with the calculated integer total magnetic moment of  $3 \mu_B/\text{cell}$ ) with a bandgap in the spin minority channel of  $\sim 2.7$  eV, cf. Fig. 3. This leads to a complete, i.e., 100 %, spin polarization of the conduction electrons and thus makes the system attractive for high-efficiency magneto-electronic devices – specifically, magnetoresistive tunnel junctions.

Based on these results, in particular on the preference of Cr atoms to substitute Ga rather than Al atoms in the AlN/GaN (0001), we model a realistic (in the sense of practical applications) magneto-electronic system using (2x2) supercells of Cr-doped graded  $\text{Al}_{1-x}\text{Ga}_x\text{N}/\text{GaN}$  (0001) heterostructures. From a comparison of the total energies for the relaxed structures with different Cr site locations, we found that the magnetic impurity prefers to substitute the Ga atoms which are located in the pure GaN (0001) layers (cf. cases 7-14 in Fig. 4). A significant total energy increase is obtained for the structures where Cr substitutes the Ga atoms in the mixed nitride (0001) layers (cf. cases 1-6 in Fig. 4). This energy dependence on the composition suggests the possibility to control the width and height of the energy barrier by adjusting the Ga/Al ratio in the layers perpendicular to the growth direction – an important ingredient for device design optimization.

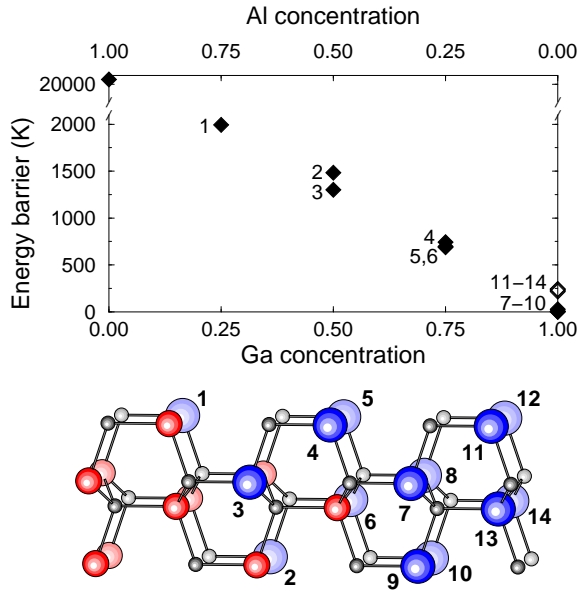


FIG. 4. Calculated relative formation energies, K, as a function of the cation concentration  $x$  in the Cr-doped graded  $\text{Al}_{1-x}\text{Ga}_x\text{N}/\text{GaN}$  (0001) heterostructures and geometry of the corresponding supercell. The numbers on the graph correspond to those in the supercell and denote the Ga site locations substituted with a Cr atom.

In summary, based on the first-principles calculations, we predict that efficient spin injection can be achieved using a ferromagnetic GaN:Cr electrode in conjunction with an AlN tunnel barrier. Since the Cr-doped AlN/GaN (0001) heterostructures are found to be half-metallic, one can expect a pronounced increase of magnetoresistance in the nitride-based magnetic tunnel junctions. These findings make the system highly attractive for spintronic applications and call for experimental investigations.

Work supported by DARPA (grant 02-092-1/N00014-02-1-05918). Computational resources provided by the NSF supported National Center for Supercomputing Applications, Urbana-Champaign.

<sup>1</sup> R. J. Soulen, Jr. *et al.*, Science **85**, 282 (1998); C. T. Tanaka, J. Nowak, and J. S. Moodera, J. Appl. Phys. **86**, 6239 (1999).

<sup>2</sup> D. Ristoiu *et al.*, Europhys. Lett. **49**, 624 (2000).

<sup>3</sup> G. A. de Wijs, and R. A. de Groot, Phys. Rev. B **64**, 020402(R) (2001); S. Picozzi, A. Continenza, and A. J. Freeman, J. Appl. Phys. **94**, 4723 (2003); A. Debernardi, M. Peressi, and A. Baldereschi, Mat. Sci. Eng. C **23**, 743 (2003); I. Galanakis, cond-mat/0408204.

<sup>4</sup> Nitride semiconductors: handbook on materials and devices, edited by P. Ruterana, M. Albrecht, and J. Neugebauer (Weinheim, Great Britain, 2003).

<sup>5</sup> T. Dietl *et al.*, Science **287**, 1019 (2000).

<sup>6</sup> H. X. Liu *et al.*, to be published in Appl. Phys. Lett.; S. Y. Wu *et al.*, Mat. Res. Soc. Symp. Proc. **798**, Y10.57 (2004); D. Kumar, J. Antifakos, M. G. Blamire, and Z. H. Barber, Appl. Phys. Lett. **84**, 5004 (2004).

<sup>7</sup> S. Krishnamurthy, M. van Schilfgaarde, and N. Newman, Appl. Phys. Lett. **83**, 1761 (2003).

<sup>8</sup> S. D. Lester *et al.*, Appl. Phys. Lett. **66**, 1249 (1995).

<sup>9</sup> M. van Schilfgaarde, and O. N. Mryasov, Phys. Rev. B **63**, 233205 (2001).

<sup>10</sup> S. E. Park *et al.*, Appl. Phys. Lett. **80**, 4187 (2002); S. G. Yang, A. B. Pakhomov, S. T. Hung, and C. Y. Wong, Appl. Phys. Lett. **81**, 2418 (2002); S. Y. Wu *et al.*, Appl. Phys. Lett. **82**, 3047 (2003).

<sup>11</sup> G. P. Das, B. K. Rao, and P. Jena, Phys. Rev. B **69**, 214422 (2004).

<sup>12</sup> Below the critical thickness of  $\sim 50$  Å for GaN layers grown on AlN (0001), both GaN and AlN have the same in-plane lattice constant; see C. Kim, I. K. Robinson, J. Myoung, K.-H. Shim, and K. Kim, J. Appl. Phys. **85**, 4040 (1999).

<sup>13</sup> E. Wimmer, H. Krakauer, M. Weinert, and A. J. Freeman, Phys. Rev. B **24**, 864 (1981).

<sup>14</sup> R. Asahi, W. Mannstadt, and A. J. Freeman, Phys. Rev. B **59**, 7486 (1999).

<sup>15</sup> We used cut-off parameters of 12.96 Ry in the wave vectors and  $\ell \leq 3$  inside the muffin-tin spheres.

<sup>16</sup> S. Strite, and H. Morkoc, J. Vac. Sci. Tech. B **10**, 1237 (1992); and references therein.

<sup>17</sup> From additional calculations for (1x1) AlN/GaN (0001) with 5 double layers of each material, we found that the difference between the bandgap values for the GaN layers and the AlN layers located further away from the junctions is 0.4 eV (1.3 eV) within the LDA (sX-LDA).

<sup>18</sup> We assume metal-rich growth conditions, i.e., the atom removed from (added to) the AlN/GaN is incorporated into (comes from) the corresponding bulk reservoir; thus, the formation energy is calculated as  $E_f = E_{\text{int:Cr}} - E_{\text{int}} - E_{\text{Ga(Al)}} + E_{\text{Cr}}$ , where  $E_{\text{int:Cr}}$ ,  $E_{\text{int}}$ ,  $E_{\text{Ga(Al)}}$ , and  $E_{\text{Cr}}$  are the total energy of the Cr-doped interface, the corresponding undoped interface, bulk orthorhombic Ga (fcc Al) and bcc Cr, respectively.

<sup>19</sup> From additional calculations of Cr-doped (2x2) AlN/GaN (0001) with 5 double layers of each material, we found a negligible variation in the formation energies ( $< 0.04$  eV) across the heterostructure.

<sup>20</sup> We also found that the Cr induced magnetic moments on its neighboring Ga atoms ( $\sim 0.014 \mu_B$ ) are larger than those on the Al atoms ( $\sim 0.010 \mu_B$ ).

<sup>21</sup> J. Kanamori, and K. Terakura, J. Phys. Soc. Japan **70**, 1433 (2001).

<sup>22</sup> Within the linear muffin-tin orbital method in the atomic sphere approximation, the effective exchange interaction parameters were calculated as a second derivative of the ground-state energy with respect to the magnetic moment rotation angle; see A. I. Liechtenstein, M. I. Katsnelson, V. P. Antropov, and V. A. Gubanov, J. Magn. Magn. Mater. **67**, 65 (1987).

<sup>23</sup> J. E. Medvedeva *et al.*, to be published.